A Downlink Load Control Scheme with a Dynamic Load Threshold and Virtual Coverage Management for Two-Tier Femtocell Networks

Chang Soon Kang[1], Tien Dung Nguyen[1], Junsu Kim[2], and Renato Lo Cigno[3]
[1]Dept. of Information and Communication Engineering,
Changwon National University, Changwon, Republic of Korea.
[e-mail: cskang@changwon.ac.kr, tiendungnguyen87@gmail.com]
[2]Dept. of Electronics Engineering,
Korea Polytechnic University, Siheung, Republic of Korea
[e-mail: junsukim@kpu.ac.kr]
[3]DISI, University of Trento, Trento, Italy
[e-mail: locigno@disi.unitn.it]
*Corresponding author: Chang Soon Kang

Received May 29, 2013; revised August 19, 2013; revised October 6, 2013; accepted November 2, 2013; published November 29, 2013

Abstract

This paper proposes a dynamic downlink load control scheme that jointly employs dynamic load threshold management and virtual coverage management schemes to reduce the degree of performance degradation due to traffic overload in two-tier femtocell networks. With the proposed scheme, the downlink load in a serving macrocell is controlled with a load threshold which is adjusted dynamically depending on the varying downlink load conditions of neighboring macrocells. In addition, traffic overloading is alleviated by virtually adjusting the coverage of the overloaded serving macrocell, based on the adjusted load threshold of the serving macrocell. Simulation results show that the proposed scheme improves the performance of two-tier femtocell networks in terms of the outage probability and sum throughput. This improvement is significantly increased with appropriate values of load thresholds and with an intermediate-level adjustment of the virtual coverage area (i.e., handover hysteresis margin: HOM). Furthermore, the proposed scheme outperforms both a previously proposed load control scheme with a static load threshold and the LTE system without a HOM adjustment.

Keywords: Load control, dynamic load threshold, femtocell, handover, virtual coverage adjustment

A preliminary version of this paper appeared in ICTC 2011, September 28-30, Seoul, Korea. This version includes a new idea with the extension of the study in the confernce paper. This research was finantially supported by Changwon National University in 2012.

http://dx.doi.org/10.3837/tiis.2013.11.003

1. Introduction

A two-tier femtocell network is considered an attractive way to improve the system capacity and quality of service in next-generation mobile communication networks. A short range, low-power, low-cost base station, the home eNodeB connects to the backhaul of an internet network and improves indoor coverage. It can be operated in closed access, open access and hybrid access modes in the licensed spectrum. Femtocells overlaid with the coverage of macrocells can be used to offload high-rate data traffic from the macrocells improving the quality of service and decreasing the probability of outages [1], [2].

Bursty traffic with high data rates has been steadily increasing with the deployment of 'beyond third-generation' cellular networks. An abrupt increase in the traffic load can cause traffic overloading situations, thereby seriously degrading the performance of cellular networks. An adaptive cell-sizing scheme was proposed in [3] to relieve the traffic load in cellular CDMA networks, in which the coverage of the serving cell and target cell is reduced and extended, respectively, by changing the transmission power of the base stations. This scheme, however, can cause coverage holes and increase the call drop rate in varying traffic load environments. A soft handover algorithm with variable thresholds was proposed to resolve the traffic non-uniformity among cells which degrades the overall system performance of cellular CDMA systems [4]. An adaptive handover algorithm for cellular WCDMA systems was studied [5], in which downlink overload traffic is transferred to neighboring cells by changing the handover parameters without adjusting the transmission power of the base stations. A downlink load control scheme was also introduced [6] to alleviate traffic overloading by dynamically changing the channel quality indicator (CQI) values based on the downlink load of the serving cell in coexisting WCDMA and HSDPA networks.

The capacity and interference in microcell and macrocell overlaid CDMA networks were investigated in [7]. In [8], a self-optimizing algorithm which tunes the handover parameters of a long-term evolution (LTE) base station was presented. Also, a handover algorithm with adaptive hysteresis margin was proposed [9], in which the hysteresis margin can be changed depending on the distance between a mobile user and the base station of the target cell, even if the cell radius commonly varies due to interference from serving and neighboring cells. In [10], an adaptive coverage adjustment approach for two-tier femtocell networks was studied, where the transmission pilot power of a serving femtocell changes based on the distance between the femtocell and the most outer user of the cell. An adaptive handover hysteresis margin scheme exploiting the fundamental idea from earlier work [9] has been presented [11], in which the hysteresis margin for femtocell networks can be adjusted according to the estimated measurement value of the signal strength and the signal-to-interference ratio received at the user equipment (UE). In addition, a traffic load adaptive power control mechanism for femtocells was proposed in [12], in which it can reduce the transmission power when the traffic load is low, while avoiding throughput degradation of femtocells. Also, an earlier work [13] studied an adaptive power control scheme for femtocells based on current traffic load and the signal quality between users and the femtocell, in which the data frames of the femtocells can be fully utilized, while meeting the quality of service (QoS) of users. These studies [7]-[13], however, have not taken into account traffic overloading issues in two-tier femtocell

networks.

A downlink load control scheme for two-tier LTE-based femtocell networks was recently investigated [14], [15], in which overloading traffic can be handed over to neighboring macrocells and femtocells by reducing the handover threshold. In these studies, the downlink traffic load is controlled with a static load threshold based solely on the traffic load of the serving macrocell, irrespective of varying downlink load situations in neighboring macrocells. Hence, the performance of two-tier femtocell networks can be seriously degraded when neighboring macrocells operate under highly loaded conditions. In addition, the signal power of mobile users can deteriorate during the handover, even if this downlink load control scheme is operating properly in the neighboring macrocells. This problem can also degrade performance levels even with the use of two-tier femtocell networks.

In this paper, we propose a new dynamic downlink load control scheme that reduces performance degradation due to overload traffic in two-tier femtocell networks. With the proposed scheme, the downlink load in the serving macrocell is controlled with a load threshold that is adjusted dynamically depending on the varying downlink load status in neighboring macrocells. Moreover, overload traffic is alleviated by changing the handover thresholds, based on the adjusted load threshold of the serving macrocell. In particular, this paper evaluates and compares the performance levels between the proposed scheme and two other schemes, i.e., a scheme with a static load threshold [14] and the LTE system [16] without an adjustment of the handover hysteresis margin, in terms of the average outage probability and sum throughput. We consider both macrocell-to-macrocell handover and macrocell-to-femtocell handover as well as the number of macrocell users and the number of femtocell deployments per macrocell. Also, we obtain the outage probability considering both the total power allocated to users in the serving macrocell and the signal strength of macrocell users received from neighboring macrocells and femtocells during handovers.

The rest of this paper is organized as follows. The system model with a two-tier LTE-based femtocell network is described in Section 2. The proposed dynamic downlink load control scheme is described in Section 3. In Section 4, simulation results of assessments of the performance and the results of the comparison are discussed in terms of the outage probability and sum throughput in the two-tier femtocell network. Finally, conclusions are drawn in Section 5.

2. System Model

We consider the downlink of the two-tier LTE-based femtocell network shown in Fig. 1, in which multiple femtocells are overlaid with macrocells and use the same spectrum as the macrocells [16]. In a macrocell network, the macrocell evolved NodeB (MeNB) can exchange traffic load information among adjacent MeNBs through X2 interfaces while the mobility management entity (MME) manages the mobility of macrocell user equipment (MUE). The home eNodeB (HeNB) components of the femtocell network are connected to a HeNB-gateway and the MME via S1 interfaces.

We assume that femtocells are uniformly distributed in macrocells and that they operate in open access mode. This means that every macrocell and femtocell user can utilize the resources of femtocells when the user stays in the femtocell zone. In addition, we assume that macrocells and femtocells provide voice and data services to mobile users.

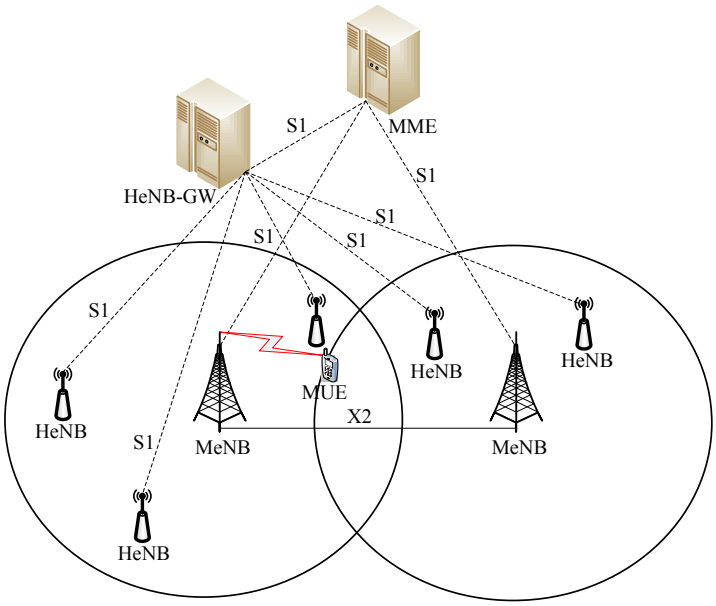

Fig. 1. A two-tier LTE-based femtocell network.

3. Dynamic Downlink Load Control Scheme

Handover decisions in the LTE system are performed with two threshold parameters; the handover hysteresis margin (HOM) and the time-to-trigger (*TTT*) timer. The HOM ensures that the target cell is the most appropriate cell for mobile users to camp on after handover, and the TTT timer restricts handover actions which are triggered within a certain time, thus offering protection from oscillating behaviors. This is formally expressed as [16]:

$$\begin{cases} RSRP_T > RSRP_S + HOM \\ HO_{Trigger} \geq TTT \end{cases} \tag{1}$$

where $RSRP_T$ and $RSRP_S$ are the reference signal received power (RSRP) from the target cell and the serving cell, respectively, and $HO_{Trigger}$ is the handover trigger timer which starts counting when the first condition in Equation (1) is satisfied.

With the handover algorithm of the LTE system without an adjustment of HOM given by Equation (1) (hereinafter referred to as the original LTE system), however, it is difficult to manage traffic overloading effectively in two-tier femtocell networks. Hence, the virtual coverage management (VCM) scheme was introduced [14], [15] to alleviate traffic overloading, where the coverage of an overloaded serving macrocell is virtually shrunk by decreasing the predefined threshold values of HOM and *TTT*. In this way, the MUEs in the serving macrocell can be easily handed over to adjacent cells. Note that with increases of the predefined handover thresholds in a serving macrocell, the coverage of the serving macrocell can be virtually expanded and the serving macrocell can thus accommodate more users flowing from other cells.

For the proposed dynamic load control scheme, a measure of the current downlink

load[1] in a macrocell k, L_k is defined as follows:

$$L_k = \frac{P_k^{alloc}}{P_k^{total}} \tag{2}$$

Here, P_k^{total} is the total power of MeNB k that can be allocated to the downlink traffic channels, and P_k^{alloc} is the current aggregated power allocated to active downlink traffic channels of MeNB k. Moreover, to classify the downlink load states of neighboring macrocells, two load thresholds are considered, L_L and L_H, which are predefined as the low and high load thresholds, respectively.

We here note that traffic load estimation based on the physical resource block (PRB) utilization can also be used for representing the load status [18]-[20]. In addition, the load status can be represented by considering the call blocking ratio [21] or the call dropping ratio [22]. This study, however, focuses mainly on our proposed downlink load control scheme for alleviating traffic overloading, while the issue of traffic load metrics is of secondary importance. PRB utilization may be a more adequate load metric, but both the *power-based load metric* defined in Equation (2) and the *PRB-based load metric* are strongly correlated from a long-term average standpoint. In particular, it is evident that regardless of how a downlink power control is operated in the two-tier network, a higher level of transmission power is required *stochastically* for a larger number of mobile users. Therefore, downlink load estimation based on the transmission power ratio, i.e., the *power-based load metric*, can also be used for representing the load status in terms of the operation and the long-term average performance of the proposed downlink load control scheme described below.

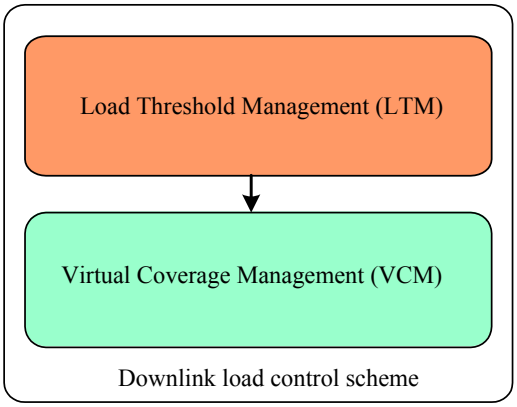

Fig. 2. Proposed downlink load control scheme for two-tier femtocell networks.

As shown in **Fig. 2**, the proposed dynamic downlink load control scheme jointly employs load threshold management (LTM) and virtual coverage management (VCM) schemes for two-tier femtocell networks, where the LTM dynamically adjusts the predefined load threshold in the serving macrocell depending on the changes in the load

[1]Even if the power allocated to each active channel is varied by the downlink power control of MeNB as in [17], to simplify and clarify conceptually the measure of downlink load in a macrocell, the issue of the varying power of the active channel is not considered.

conditions of neighboring macrocells[2]. With the LTM, the downlink load control scheme broadcasts a handover threshold update message to the MUEs in an overloaded serving macrocell (**Fig. 3**).

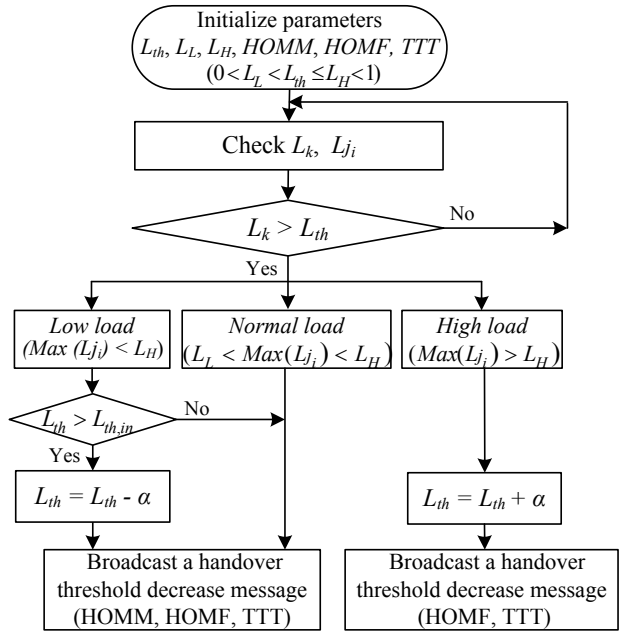

Fig. 3. Load threshold management in the proposed downlink load control scheme.

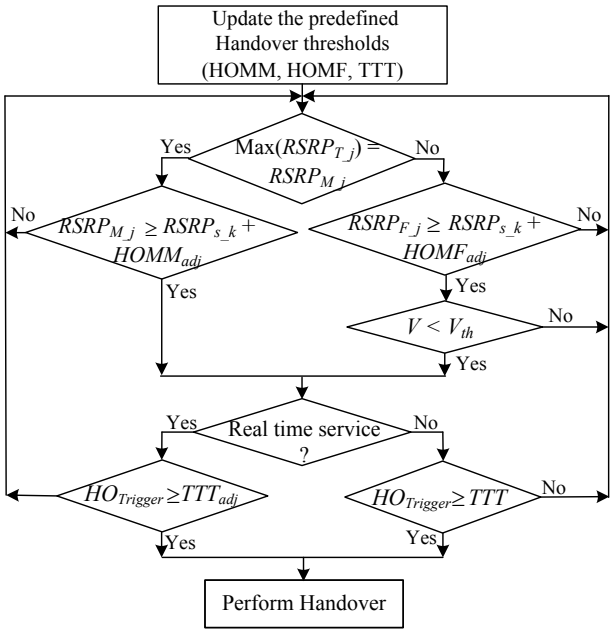

Fig. 4. Virtual coverage management in the proposed downlink load control scheme.

[2]To decrease the computational complexity of the proposed scheme, the load threshold of the serving macrocell is adjusted by considering only the downlink load status of the neighboring macrocells, even if an MUE has a possibility to handover from a macrocell to an overloaded femtocell.

The VCM is activated by receiving the update message at mobile users when the serving macrocell is overloaded. In this manner, the coverage of the serving macrocell is virtually shrunk by changing (i.e., decreasing) the handover threshold values. In other words, the handover zone of MUEs in the serving macrocell is virtually expanded (**Fig. 4**). Note that cell coverage is *virtually* adjusted by changing the handover threshold values of mobile users without changing the transmission power of the base stations. This is referred to as VCM henceforth, even if the VCM is directly related to the handover decision. Also, note that the transmission power of base stations is not changed by the VCM, and thus the cell radius is not *really* changed regardless of changing the handover threshold values.

With the LTM, when the downlink load of a serving macrocell L_k exceeds a predefined load threshold identifying an overload situation, the load threshold in the serving macrocell is dynamically adjusted in different ways depending on the following three downlink load states Lj_i of the neighboring macrocells: a low-load state, normal-load state, and high-load state.

If the traffic loads in all of the neighboring macrocells are low (i.e., $Max(Lj_i) < L_L$), the predefined load threshold is then adjusted differently according to the load threshold value established in the serving macrocell. When the load threshold set in a serving macrocell k, L_{th}, is equal to the predefined load threshold in the serving macrocell ($L_{th,in}$), the load threshold is not changed. In contrast, if the load threshold established in the serving macrocell k is greater than the predefined load threshold, then the established load threshold, L_{th}, is decreased by α. After adjusting the load threshold, the VCM is employed for the overloaded serving macrocell. That is, the serving MeNB transmits a handover thresholds update message to all of the MUEs, decreasing the handover thresholds to favor outbound handovers. Hence, the handovers of the MUEs from the overloaded macrocell to the neighboring cells are effectively advanced when compared to the other two load states, where the neighboring cells include the femtocells overlaid with the serving macrocell as well as the neighboring macrocells and femtocells.

In the normal-load state (i.e., $L_L < Max(Lj_i) < L_H$), a static load threshold is implemented for load threshold management despite the fact that the VCM is applied for an overloaded serving macrocell in the same manner used for a low-load state. In the low-load and normal-load states, the handover thresholds for the VCM consist of *HOMM* (HOM for macrocells), *HOMF* (HOM for femtocells), and *TTT*.

On the other hand, when the downlink load in neighboring macrocells approaches a high load state; that is, when one of the neighboring macrocells is heavily loaded, (i.e., $Max(Lj_i) > L_H$), the predefined load threshold of the serving macrocell, L_{th}, is increased by α. However, in this load state, even if the VCM is employed for the overloaded serving macrocell, only *HOMF* and *TTT*, and not *HOMM*, are adjusted (i.e., decreased) for the MUEs in the serving macrocell.

Note that with the proposed scheme, in cases with low-load and normal-load states, overloading traffic in a serving macrocell can be alleviated by macrocell-to-femtocell handovers[3] and by macrocell-to-macrocell handovers. On the other hand, for a high-load state, overloading traffic can be relieved mainly by femtocells overlaid with an overloaded serving macrocell, in which macrocell-to-femtocell handovers are preferable and macrocell-to-macrocell handovers are delayed when compared to the other load states. Furthermore, note that the dynamic load threshold in the proposed scheme is adaptively

[3] Femtocell-to-macrocell and femtocell-to-femtocell handovers are beyond the scope of this study, where we do not consider the issue of the offloading from femtocells to other cells.

adjusted depending on the changes in the downlink traffic load of neighboring macrocells, whereas the static load threshold proposed in the aforementioned study [14] is not changed regardless of the traffic load conditions of the neighboring macrocells.

In particular, with the VCM, when the MUEs in the serving macrocell receive a handover threshold decrease message, they update their predefined handover thresholds with new thresholds as follows:

$$HOMM_{adj} = HOMM - \Delta HOM \tag{3}$$

$$TTT_{adj} = TTT - \Delta TTT \tag{4}$$

$$HOMF_{adj} = HOMF - \Delta HOM \tag{5}$$

Here, ΔHOM, ΔTTT, $HOMM_{adj}$, $HOMF_{adj}$ and TTT_{adj} are the decrements of HOM and TTT and the handover thresholds adjusted by the decrements, respectively. With TTT_{adj}, the handover of real-time traffic to femtocells can be quickly determined, and the latency time can be reduced. Because deferring an impending handover for a long time may lead to call drops, decreasing the value of TTT is suitable for real-time applications. In contrast, for non-real-time applications, a handover delay is tolerable.

Meanwhile, the MUEs in the serving macrocell monitor the signal strength from neighboring cells after updating their handover thresholds and attempt to make handovers to adjacent macrocells or femtocells with the best RSRP values. In Fig. 4, $RSRP_{s\_k}$, $RSRP_{T\_j}$, $RSRP_{M\_j}$, and $RSRP_{F\_j}$ are the RSRP values from the serving macrocell k, the target cell j, the neighboring macrocell (MeNB) j, and the femtocell (HeNB) j, respectively, and V_{th} is the velocity threshold of the MUEs, i.e., the speed[4] above which MUEs will not attempt a handover to a femtocell because the dwell time there would be too small given the size of the femtocell coverage [24]. When mobile users in the serving macrocell select the neighboring femtocell with the strongest signal strength, they attempt to make handovers based on the handover conditions with $HOMF$ instead of HOM in Equation (1).

4. Performance Evaluation

In this section, we discuss simulation results of assessments of the performance and the results of the comparison between the proposed scheme and two other schemes, i.e., a scheme with a static load threshold [14] and the LTE system [16] without a HOM adjustment in the two-tier femtocell network.

4.1. Evaluation Methodology

The performance of the proposed dynamic load control scheme is evaluated for a two-tier LTE-based femtocell network with various parameters, as shown in Table 1. The two-tier femtocell network consists of seven omni-macrocells that are overlaid with femtocells. The inter-site distance between two MeNBs is 1.5 *km*, and they are disposed in the center of overlapping circular cells. The macrocells operate at 2 *GHz* with a 5 *MHz* bandwidth divided into 25 RBs (Resource Block) and the femtocells use the same spectrum as the macrocells. Each HeNB can support a maximum of four users and operates in open-access mode; a MUE entering a femtocell will remain there until its call ends.

[4] The velocity of MUEs can be obtained by speed estimators as in [23, 24].

Table 1. Simulation parameters.

Parameter		Value
System	carrier frequency, bandwidth	*2 GHz, 5 MHz*
	MeNB, HeNB antenna pattern	omni-directional
	number of RBs	*25*
	number of sub-carrier per RB	*12*
	RSRP sampling time interval	*50 msec*
	packet schedule	proportional fair
	TTI	*1 msec*
	α	*0.1*
Macrocell	radius	*1 Km*
	inter-site distance	*1.5 Km*
	MeNB TX power	*43 dBm*
Femtocell	radius	*30 m*
	HeNB TX power	*20 dBm*
Handover parameters	*HOMM, HOMF, ΔHOM*	*3 dB, 1 dB, 0.5 dB*
	TTT, ΔTTT	*100 msec, 20 msec*
Mobility and traffic types	V_{th}	*10 km/h*
	moving direction	*[0, 360⁰]*
	real-time (VOIP), ratio	*12.2 kbps, 70 %*
	non-real-time (WWW), ratio	*128 kbps, 30 %*
Channel Model	path-loss	ITU-R outdoor
	log-normal shadowing (mean, standard deviation)	*(0, 8 dB)*

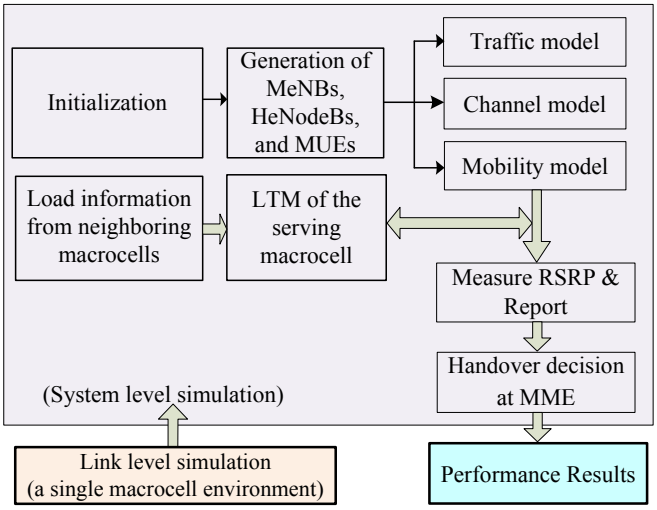

Fig. 5. Simulator structure of the proposed load control scheme.

The proposed scheme has been implemented in a simulation with CSIM [25] considering both link-level and system-level characteristics, as shown in Fig. 5. The performance of the proposed scheme is compared to that of a) a scheme with a static load threshold, and b) the original LTE system without a HOM adjustment. We assume that femtocells are uniformly distributed in macrocells. In addition, MUEs are uniformly distributed in every macrocell and constantly move at a fixed speed; 80 percent of the MUEs travel at speeds which are lower than the velocity threshold V_{th}. MUEs in a serving macrocell and neighboring macrocells travel in random directions that range from 0 to

360 degrees. The number of MUEs is randomly changed from 150 to 400 users to consider different traffic load situations in each macrocell. The following parameters, $\alpha = 0.1$, $L_{th} = 0.7$, $L_L = 0.4$, and $L_H = 0.7$ [26] are set as the predefined load thresholds[5] for the load threshold management, the adjustment value of the load threshold in a serving macrocell, and the two load thresholds of the neighboring macrocells, respectively.

Both macrocell-to-macrocell handovers and macrocell-to-femtocell handovers are enabled. Note that α = 0.1 means a 10 percent adjustment in the total downlink load of an overloaded serving macrocell. A larger value of α can affect the stability of the two-tier femtocell network; thus, we use the adjustment value considering the handover probability of approximately 0.1 when L_{th} = 0.7 and ΔHOM = 0.5 *dB* (refer to Fig. 7). Moreover, note that L_{th} = 0.7 means the macrocell becomes overloaded with traffic when 70 percent of the total downlink power is allocated to users in the serving macrocell.

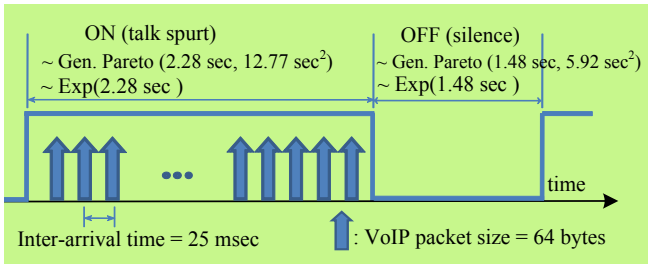

Fig. 6. A VoIP (ON/OFF) traffic model for real-time service.

The propagation channel model is considered with path-loss, shadowing, and Rayleigh fading, in which the outdoor model of ITU-R [27] is used for the path-loss characteristic and a standard deviation of 8 *dB* is set for shadowing. During the MUE calls, path-loss between the MeNB and the MUEs is constant. We use the 16 CQI values defined in [28] with target block error rates determined in our link-level simulation. Each CQI value is reported to the MeNB during each time-to-interval (TTI) period of 1 millisecond (*msec*).

We consider that macrocells and femtocells provide voice-over-internet protocol (VoIP) traffic for real-time service and worldwide web (WWW) traffic[6] for non-real-time service. The VoIP traffic follows an ON/OFF traffic model, where the ON/OFF periods are modeled as a generalized Pareto distribution, as shown in Fig. 6. The mean and variance for the ON/OFF periods are respectively (2.2882, 12.77) and (1.4849, 5.9242) [29]. Voice packets with a size of 64 bytes are generated every 25 *msec* within each ON period [30]. The mean data rates of the VoIP and web traffic are approximately 12.2 *kbps* and 128 *kbps*, respectively. The initial locations of the MUEs are uniformly distributed in each macrocell irrespective of each user's service type.

4.2. Simulation Results

We first examine the performance of the proposed dynamic load control scheme according to ΔHOM and L_{th}.

[5] The issue of determining the predefined low and high load thresholds in detail, i.e., L_L and L_H, is remained as further study.

[6] Even if the MUEs are uniformly distributed in macrocells with varying number of mobile users, a bursty traffic model which generates abruptly increasing traffic instantaneously is suitable to evaluate the *effectiveness* of the proposed scheme against traffic overloading situations.

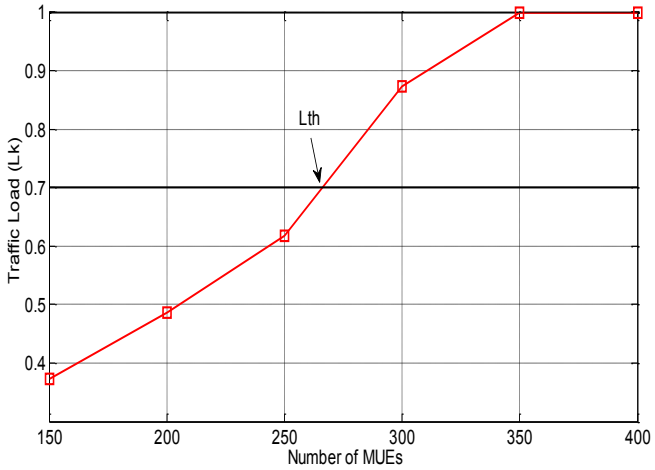

Fig. 7. Traffic load of the serving macrocell according to the number of MUEs.

Note that delta HOM hereinafter means Δ*HOM* in the following figures. Fig. 7 shows downlink traffic load of the serving macrocell in the two-tier femtocell network. When the downlink traffic load in the serving macrocell is 0.7, the number of MUEs in the macrocell approaches approximately 270 [14]. Hence, when the number of users in the serving macrocell exceeds 270, the proposed load control scheme is applied to the two-tier femtocell network.

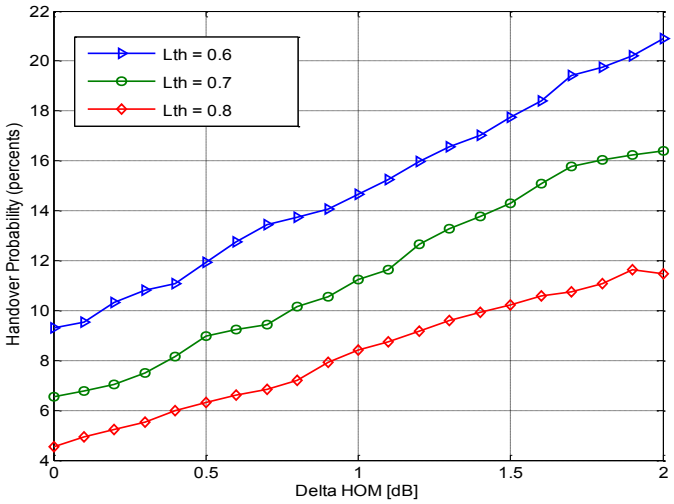

Fig. 8. Handover probability from a serving macrocell to neighboring cells according to Δ*HOM* and L_{th} (300 MUEs are given).

Fig. 8 shows the average handover probability from a serving macrocell to its overlaid femtocells as well as the neighboring macrocells and femtocells according to a predefined load threshold value of L_{th} and a decrement value of HOM (i.e., Δ*HOM*). As the Δ*HOM* value increases, the coverage of the serving macrocell is virtually reduced. Specifically, the criterion for handover decisions is relaxed by decreasing the threshold HOM in Equation (1). Hence, the handover probability increases almost linearly with an increase of the Δ*HOM* value, specifically, with decreases of $HOMM_{adj}$ and $HOMF_{adj}$ in Equations (3) and (5), respectively. In contrast, as the load threshold (L_{th}) increases, the number of

handover users from the serving macrocell to neighboring cells decreases. As a result, the handover probability is also reduced.

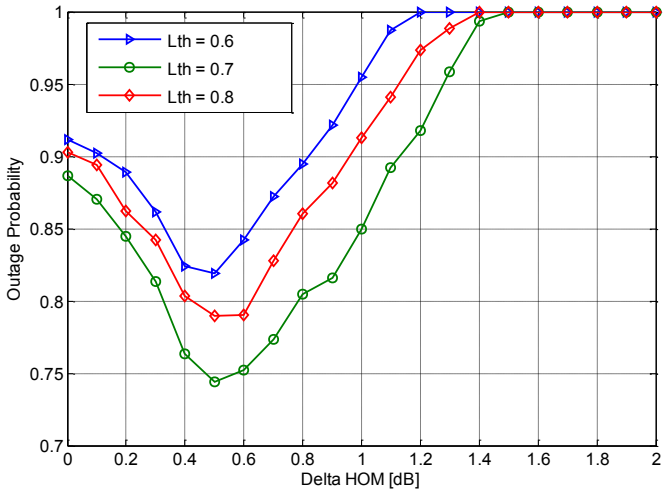

Fig. 9. Outage probability of a serving two-tier femtocell network depending on ΔHOM (with 300 MUEs).

Fig. 9 shows the average outage probability of a serving two-tier femtocell network for the HOM adjustment level. The serving two-tier femtocell network hereinafter means the serving macrocell and its overlaid femtocells. The outage probability P_{out} of the proposed scheme is obtained by Equation (6).

$$\begin{aligned} P_{out} &= P_{out}^{real} + P_{out}^{non-real} \\ &= \Sigma[(P_{out}^{pow} + P_{out}^{sig})(R_{real} + R_{non-real})] \end{aligned} \tag{6}$$

Here, P_{out}^{real} and $P_{out}^{non-real}$ are the average outage probabilities of real-time and non-real-time traffic, respectively. Additionally, R_{real} and $R_{non-real}$ are the ratios of the real-time traffic and non-real-time traffic, respectively, and $R_{real} + R_{non\text{-}real} = 1$. In Equation (6), P_{out}^{pow} denotes the *ratio of time* in which the total power allocated to MUEs in the serving MeNB exceeds the predefined load threshold during the simulation time, and P_{out}^{sig} is *the ratio of time* in which the signal strength of MUEs received from the neighboring macrocells and femtocells is lower than -120 *dBm* and -70 *dBm*, respectively, during the handovers in the simulation time. Note that the outage probability by the received signal strength is related to both macrocell-to-macrocell and macrocell-to-femtocell handover failures.

We here note that a UE can undergo an outage if the signal strength received from a cell drops under a certain threshold regardless of whether the UE is served by a macrocell or a femtocell. In this study, however, we focus on our proposed downlink load control scheme for alleviating traffic overloading by the VCM when a serving macrocell is overloaded. With the VCM, MUEs in the serving macrocell can be handed over to neighboring femtocells or macrocells. In particular, *immediately after* completing the process of a macrocell-to-femtocell handover, a MUE handed over to a femtocell can also experience strong interference from a heavily loaded macrocell (i.e., the old serving cell) and from other

neighboring cells. Thus, even when the MUE has '*successfully*' completed the handover process to the femtocell, the signal strength of the user received from the femtocell (i.e., the new serving cell) can rapidly drop below a criterion for handover failures, i.e., the outage threshold for femtocells. Therefore, in order to ensure the success (or failure) of macrocell-to-femtocell handovers, we assume *conservatively* an outage threshold of femtocells (i.e., -70 *dBm*) which is significantly higher than that of macrocells (i.e., -120 *dBm*), taking into account the strong macrocell interference, the small femtocell size, and the different radio propagation characteristics of macrocell and femtocell channels i.e., a heavy scattering and a line-of-sight, respectively.

The outage probability of the proposed scheme deteriorates with a larger decrement of ΔHOM, e.g., when ΔHOM is larger than about 1 *dB*. On the other hand, the outage probability can be reduced significantly when virtual coverage adjustments are intermediate in scale (e.g., ΔHOM = 0.5 *dB*), as large-scale adjustments of the virtual coverage area with a larger decrement of ΔHOM can create coverage holes at the cell edges (i.e., handover zones) between a serving macrocell and adjacent macrocells and femtocells. Furthermore, the outage probability of the proposed scheme shows an improvement as compared to cases when ΔHOM = 0 *dB*. In particular, this improvement increases when ΔHOM and L_{th} are equal to about 0.5 *dB* and 0.7, respectively. For example, with the proposed scheme, the improvement is about 10 percent when L_{th} = 0.6 and 15 percent when L_{th} = 0.7.

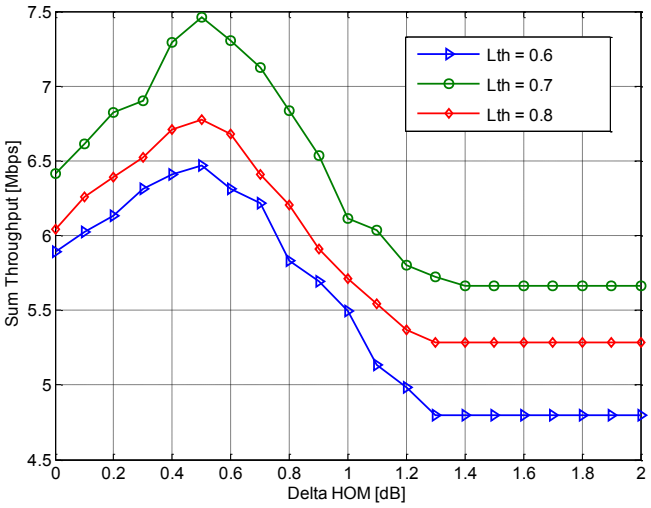

Fig. 10. Sum throughput of a serving two-tier femtocell network for ΔHOM (with 300 MUEs).

Fig. 10 shows the average sum throughput of the proposed scheme in a serving two-tier femtocell network, which is obtained as the aggregated data rates of successfully transmitted real-time and non-real-time traffic in the serving macrocell and its overlaid femtocells. With smaller values of ΔHOM (e.g., values of less than 1 *dB*), the sum throughput is improved compared to when ΔHOM = 0 *dB*. In particular, this improvement increases considerably when ΔHOM and L_{th} are equal to approximately 0.5 *dB* and 0.7, respectively. However, the sum throughput decreases considerably with a larger value of ΔHOM (e.g., ΔHOM = 1 *dB*). This result can be understood via an analogy shown in **Fig. 9**.

The performance of the proposed scheme with a dynamic load threshold is hereinafter compared with those of both the previous scheme with a static load threshold [14] and the original LTE system without a HOM adjustment; the performance metrics considered are the average outage probability and the sum throughput. A predefined load threshold (L_{th}) value of 0.7 and a ΔHOM value of 0.5 *dB* are set for the simulations of both the proposed scheme and the scheme with a static load threshold, while $\Delta HOM = 0$ *dB* corresponds to the original LTE system. We use 300 femtocell deployments per macrocell [31] for the performance comparisons.

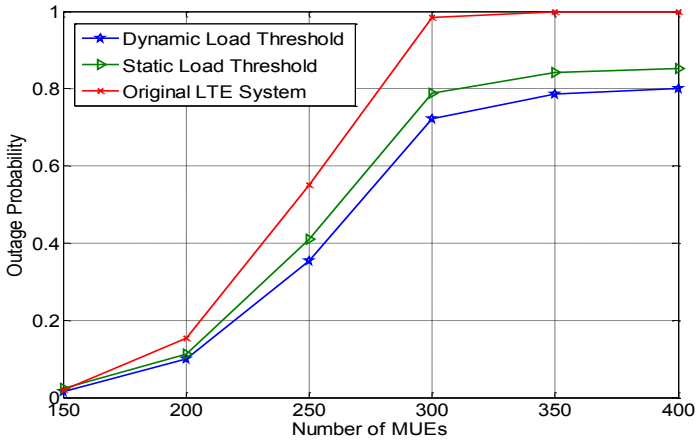

Fig. 11. Outage probability of a serving two-tier femtocell network according to the number of MUEs.

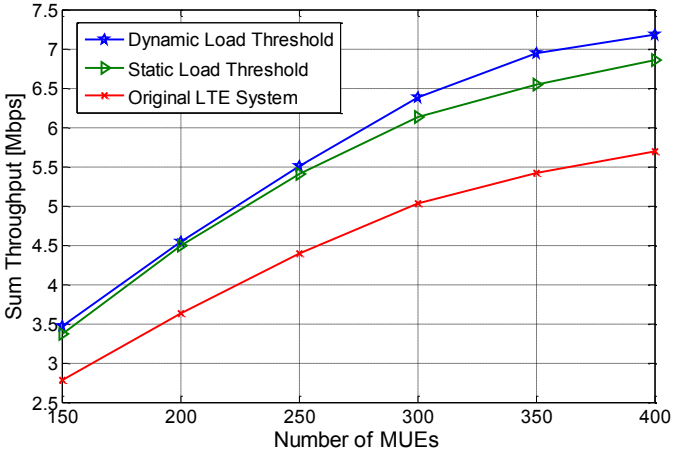

Fig.12. Sum throughput of a serving two-tier femtocell network according to the number of MUEs.

Fig. 11 shows the average outage probabilities of the proposed scheme, the previous scheme and the original LTE system in the two-tier femtocell network. The outage probability of the proposed dynamic load control scheme shows an improvement compared to the outage probabilities of both the previous scheme and the original LTE system (i.e., $\Delta HOM = 0$ *dB*). For example, with the proposed scheme, with 270 MUEs in the serving macrocell, the improvement is about 5 percent in the previous scheme and 20 percent in the original LTE system. However, in the previous scheme, MUEs in an

overloaded serving macrocell were assumed to be successfully handed over to neighboring macrocells or femtocells whenever the MUEs are satisfied with the handover conditions adjusted with new thresholds (refer to the Equations in (3), (4) and (5)), irrespective of the signal strength of the neighboring cells received at the MUEs during the handovers. That is, the outage probability in the previous scheme was obtained without consideration of P_{out}^{sig} in Equation (6). Hence, the differences in the outage probability between the proposed and the previous schemes are effectively greater than 5 percent, as described above.

Fig. 12 shows the sum throughput of a serving two-tier femtocell network, as obtained as the aggregated data rates of successfully transmitted real-time and non-real-time traffic in the serving macrocell and its overlaid femtocells. The sum throughput of the proposed scheme is considerably improved compared to the corresponding values of the other two schemes. For example, with the proposed scheme, with 300 MUEs, the improvement in the sum throughput is about 300 *kbps* compared to the corresponding value of the scheme with a static load threshold and 1.4 *Mbps* compared to that of the original LTE system.

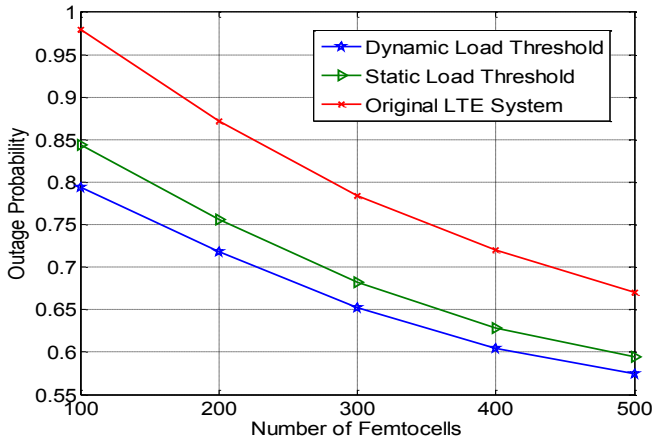

Fig. 13. Outage probability of a serving two-tier netwok depending on the number of femtocells per macrocell (with 300 MUEs).

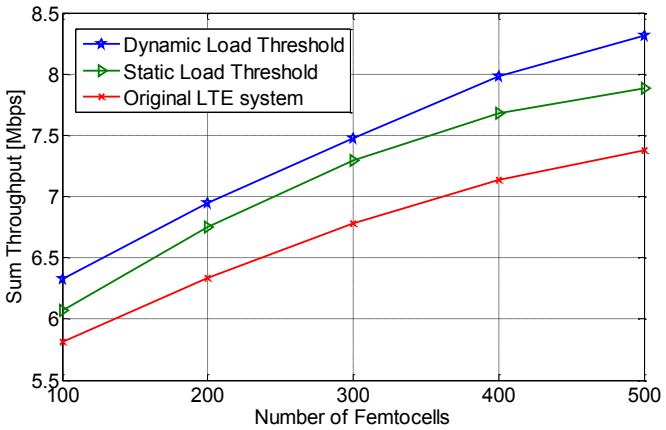

Fig. 14. Sum throughput of a serving two-tier femtocell network with the number of femtocells per macrocell (with 300 MUEs).

Fig. 13 shows the outage probability of a serving two-tier femtocell network depending on the number of femtocell deployments per macrocell. The outage probability is reduced as the number of femtocell deployments per macrocell is increased. In particular, the outage probability of the proposed scheme shows an improvement over that of the original LTE system. For example, with the proposed scheme, the improvement is increased by approximately 14 percent when the number of femtocell deployments per macrocell is 300.

Fig. 14 illustrates the sum throughput of a serving two-tier femtocell network as a function of the number of femtocell deployments per macrocell. The proposed scheme achieves enhanced sum throughput when compared to the other two schemes. This enhancement is increased with a high density of femtocell deployments. For example, with the proposed scheme, with 300 femtocell deployments per macrocell, the enhancement in the sum throughput is approximately 10 percent (i.e., 750 *kbps*) over the original LTE system. **Figs. 13** and **14** demonstrate that with the proposed load control scheme, femtocells can effectively provide a *load shelter* to users of overloaded macrocells in the two-tier femtocell network.

5. Conclusion

This paper has proposed a dynamic downlink load control scheme that reduces performance degradation due to downlink overload traffic in two-tier femtocell networks. The proposed scheme jointly employs dynamic load threshold management and virtual coverage management schemes, in which a predefined load threshold in a serving macrocell is dynamically adjusted in different ways depending on the changes in the downlink load situations of neighboring macrocells. In addition, overload traffic is alleviated by virtually adjusting the coverage of the overloaded serving macrocell with changes in predefined handover thresholds based on the adjusted load threshold of the serving macrocell.

We investigated the performance of the proposed scheme in terms of the outage probability and sum throughput in a two-tier LTE-based femtocell network. Simulation results showed that the proposed scheme enhances the sum throughput and reduces the outage probability of the two-tier femtocell network, even under heavy load conditions. In particular, this enhancement is significantly increased with appropriate values of load thresholds and intermediate-level adjustments of the virtual coverage area. Furthermore, the proposed dynamic load control scheme outperforms, in terms of the outage probability and the sum throughput, both the previous scheme with a static load threshold and the LTE system without a HOM adjustment.

References

[1] V.Chandrasekhar, J.G. Andrews, and Gatherer, "Femtocell networks: a survey," *IEEE Commun. Mag.,* vol.46, no. 9, pp.59-67, Sept. 2008. Article (CrossRefLink)

[2] D. Calin, H. Claussen, and H. Uzunalioglu "On femto deployment architectures and macrocell offloading benefits in joint macro-femto deployments." *IEEE Commun. Mag.,* Vol.48, No.1, pp. 26-32, Jan. 2010. Article (CrossRefLink)

[3] X.H. Chen, "Adaptive traffic-load shedding and its capacity gain in CDMA cellular systems," *IEE Proc.-Commun*., pp. 186-192, June 1995. Article (CrossRefLink)

[4] S.-H. Hwang, S.-L. Kim, H.-S. Oh, C.-E. Kang and J.-Y. Son, "Soft handover algorithm with variable thresholds in CDMA cellular systems," *Electron. Lett.*, vol. 33, no. 19, pp. 1602-1603, Jan.

1997. Article (CrossRefLink)
[5] W.-I. Kim and C. S. Kang, "An adaptive soft handover algorithm for traffic load shedding in the WCDMA mobile communication system," in *Proc. of WCNC 2003*, vol. 2, March 2003, pp. 1213-1217. Article (CrossRefLink)
[6] C. S. Kang, J. S. Kim, and D. K. Sung, "A dynamic downlink load control scheme for WCDMA and HSDPA system," *IEICE Trans, Commun*, vol.E92-B, No.6, pp. 2327-2331, June 2009. Article (CrossRefLink)
[7] C. S. Kang, H. S. Cho, and D. K. Sung, "Capacity analysis of spectrally overlaid macro/micro cellular CDMA systems supporting multiple types of traffic," *IEEE Trans. on Veh. Technol.*, vol. 52, no. 2, pp. 333- 346, March 2003. Article (CrossRefLink)
[8] Jansen, T. Balan, Turk, J. Moerman, I.. and Ku, rner,T., "Handover parameter optimization in LTE self- organization networks," in *Proc. of IEEE VTC 2010-Fall*, Oct. 2010, pp. 1-5. Article (CrossRefLink)
[9] S. Lal and D. K. Panwar, "Coverage analysis of handoff algorithm with adaptive hysteresis margin," in *Proc. of ICIT 2007*, Dec. 2007, pp.133 – 138. Article (CrossRefLink)
[10] S. Y. Choi, T.-J. Lee, M. Y. Chung, and H. Choo, "Adaptive coverage adjustment for femtocell management in a residential scenario," in *Proc. of APNOMS 2009*, Sept. 2009, pp. 221-230. Article (CrossRefLink)
[11] Z. Becvar and P. Mach, "Adaptive hysteresis margin for handover in femtocell networks," in *Proc. of ICWMC2010,* Sept. 2010, pp. 256–261. Article (CrossRefLink)
[12] S. Y. Yun, D.H. Cho, "Traffic density based power control scheme for femto AP," in *Proc. of IEEE PIMRC 2010*, pp. 1378-1383, Istanbul, Sept. 2010. Article (CrossRefLink)
[13] P. Mach and Z. Becvar, "QoS-Guaranteed Power Control Mechanism Based on the Frame Utilization for Femtocells," *EURASIP Journal on Wireless Communications and Networking* 2011. Article (CrossRefLink)
[14] Nguyen T. D. and C. S. Kang, "A dynamic downlink load control scheme with virtual coverage adjustments for two-tier LTE systems, " in *Proc. of ICTC2011*, pp. 487-492, Seoul, Sept. 2011. Article (CrossRefLink)
[15] C. S. Kang and Nguyen T. D., "An ecosystem-based load control scheme with virtual coverage adjustments for two-tier femtocell networks," in *Proc. of ICTC201*, Seoul, Sept. 2011, pp. 182-187. Article (CrossRefLink)
[16] 3GPP, *Radio Resource Control (RRC); Protocol specification*, TS 36.331 V10.0.0.
[17] Erik Dahlman, Stefan Parkvall, Johan Skold, and Per Beming, "3G Evolution: HSPA and LTE for Mobile Broadband," Academic Press (2007), pp. 289-298.
[18] P. Szilagyi, Z. Vincze and C. Vulkan, "Enhanced Mobility Load Balancing Optimization in LTE," in *Proc. of IEEE PIMRC 2012*, pp. 997-1003, Sept. 2012. Article (CrossRefLink)
[19] I. Siomina and D. Yuan, "Load Balancing in Heterogeneous LTE: Range Optimization via Cell Offset and Load-Coupling Characterization," in *Proc. of IEEE ICC 2012*, pp. 1357-1361, June 2012. Article (CrossRefLink)
[20] T. Warabino, S. Kaneko, S. Nanba and Y. Kishi, "Advanced Load Balancing in LTE/LTE-A Cellular Network," in *Proc. of IEEE PIMRC 2012*, pp. 530-535, Sept. 2012. Article (CrossRefLink)
[21] P. Munoz, R. Barco, J. M. Ruiz-Aviles, I. de la Bandera, and A. Aguilar, "Fuzzy Rule-Based Reinforcement Learning for Load Balancing Techniques in Enterprise LTE Femtocells," *IEEE Trans. on Veh. Technol.*, vol. 62, no. 5, pp. 1962-1973, June 2013. Article (CrossRefLink)
[22] P. Munoz, R. Barco, D. Laselva, and P. Mogensen, "Mobility-Based Strategies for Traffic Steering in Heterogeneous Networks," *IEEE Commun. Mag.*, vol. 51, no. 5, pp. 54-62, May 2013. Article (CrossRefLink)
[23] C. Tepedelenlioglu and G. B. Giannakis, "On velocity estimation and correlation properties of narrow-band mobile communication channels, "*IEEE Trans. Veh. Technol.*, vol. 50, no. 4, pp. 1039-1052, July 2001. Article (CrossRefLink)
[24] A. H. Zahran, B. Liang, and A. Saleh, "Signal threshold adaptation for vertical handoff in heterogeneous wireless networks, "*Journal of Mobile Networks and Applications*, vol.11, no. 4, pp.

625-640, August 2006. Article (CrossRefLink)
[25] Mesquite Software, Inc., *CSIM19 Simulation Engine (C Version*), Austin, TX 78755-0306.
[26] O. Blume, H. Eckhardt, S. Klein, E. Kuehn, and W. M. Wajda, ‘‘Energy savings in mobile networks based on adaptation to traffic statistics,’’ *Bell Labs Tech. J.*, vol. 15, no. 2, pp. 77–94, Sept. 2010. Article (CrossRefLink)
[27] ITU-R M.1225, “*Guidelines for the evaluation of radio transmission technologies for IMT-2000*,” 1997.
[28] H. Holma and A. Toskala, *LTE for UMTS-OFDMA and SC-FDMA Based Radio Access*, John Wiley &Son Ltd., 2009.
[29] D. Trang, B. Sonkoly, and S. Molnar, “Fractal analysis and modeling of VoIP traffic,” in *Proc. of NETWORKS2004*, June 2004, pp. 123–130. Article (CrossRefLink)
[30] Z. Bakhti and S. S. Moghaddam, “Inter-cell interference coordination with adaptive frequency-reuse for VoIP and data traffic in downlink of 3GPP-LTE,” in *Proc. of AICT 2010,* Oct. 2010, pp. 1-6. Article (CrossRefLink)
[31] R. Q. Hu, Y. Qian, and C. Q. Li, “Spectrum and energy efficient heterogeneous wireless networks,” in *Proc. of Tutorial (T5), WCNC 2013*, Shanghai, April 2013.

Chang Soon Kang received his B.S. degree from Kyungpook National University in 1984, M.S. degree from Yonsei University, Seoul, Korea, in 1986, all in electronics engineering, and Ph.D. degree in electrical engineering and computer science from the Korea Advanced Institute of Science and Technology in 2001. He joined the Electronics and Telecommunications Research Institute (ETRI), Taejon, in October 1989, where he was involved in several projects. From 1989 to 1996, he was engaged in the development of the IS-95 based CDMA Cellular System. From 1997 to 1998, he worked on a CDMA based wireless local loop system. He was also involved in developing the WCDMA based IMT-2000 system and Wireless Broadband Internet system (WiBro) from January 1999 to February 2003. In 2003, he joined a faculty member of the Changwon National University, where he is an Associate Professor in the Department of Information & Communication Engineering. From September 2012 to August 2013, he was with the Department of Computer Science and Telecommunications (DISI) of the University of Trento, Trento, Italy, as a Visiting Scholar. His research interests are in the areas of wireless communications and networks with typical emphasis on radio resource management, hierarchical cellular systems, green wireless networks, and machine-to-machine (M2M) communications.

Tien Dung Nguyen received his B.Sc. degree in electronics and telecommunication engineering from the Ho Chi Minh City University of Technology (HCMUT), Vietnam, in 2010, and M.S. degree in information and communication engineering from Changwon National University, Changwon, Korea in 2012. He was involved in the development of the simulator for M2M-based ship collision avoidance systems. His research interests include 4G mobile communication systems, Heterogeneous networks, and M2M technologies.

Junsu Kim received the B.S., M.S., and Ph.D. degrees in electric engineering and computer science from the Korea Advanced Institute of Science and Technology (KAIST), Daejeon, Korea, in 2001, 2003, and 2009, respectively. From March 2009 to August 2009, he was a Postdoctoral Research Fellow sponsored by BK21 (Brain Korea 21) with KAIST. From October 2009 to August 2011, he was a Postdoctoral Fellow with the University of British Columbia (UBC), Vancouver, BC, Canada. Since September 2011, he has been with the Korea Polytechnic University (KPU), Siheung, Korea, where he is currently an Assistant Professor. His research interests include radio resource management, wireless scheduling algorithms, cognitive radio systems, cooperative diversity techniques, and physical layer security.

Renato Lo Cigno is Associate Professor at the Department of Computer Science and Telecommunications (DISI) of the University of Trento, Italy, where he leads a research group in computer and communication networks. He received a degree in Electronic Engineering with a specialization in Telecommunications from Politecnico di Torino in 1988, the same institution where he worked until 2002. From June 1998 to February 1999, he was with the Computer Science Department, University of California, Los Angeles, as a Visiting Scholar. His current research interests are in performance evaluation of wired and wireless networks, modeling and simulation techniques, congestion control, P2P networks and networked systems in general. Renato Lo Cigno is member of IEEE and ACM and has co-authored more than 130 papers all in international, peer reviewed venues.